


Disclaimer/Publisher's Note: The statements, opinions, and data contained in all publications are solely those of the individual author(s) and contributor(s) and not of MDPI and/or the editor(s). MDPI and/or the editor(s) disclaim responsibility for any injury to people or property resulting from any ideas, methods, instructions, or products referred to in the content.

Article

Multi-criterion Sampling Matting Algorithm via Gaussian Process

Yuan Yang ^{1,†,‡} , Hongshan Gou ^{1,‡}, Mian Tan ^{1,*}, Fujian Feng ^{1,*}, Yihui Liang ², Yi Xiang ³, Lin Wang ¹ and Han Huang ³

- ¹ Guizhou Key Laboratory of Pattern Recognition and Intelligent System, Guizhou Minzu University, Guiyang, 550025, China; 380867698@QQ.com.
- ² School of Computer Science, Zhongshan Institute, University of Electronic Science and Technology of China, Zhongshan, 528400, China.
- ³ Key Laboratory of Big Data and Intelligent Robot (SCUT), MOE of China, School of Software Engineering, South China University of Technology, Guangzhou 510006, China.
- * These authors should be considered co-corresponding authors: tanmian@gzmu.edu.cn (Mian Tan); fujian_feng@gzmu.edu.cn (Fujian Feng).
- † Current address: Guizhou Minzu University, Guiyang.
- ‡ These authors contributed equally to this work.

Abstract: Natural image matting is an essential technique for image processing that enables various applications, such as image synthesis, video editing, and target tracking. However, the existing image matting methods may fail to produce satisfactory results when computing resources are limited. Sampling-based methods can reduce the dimensionality of the decision space and therefore reduce computational resources by employing different sampling strategies. While these approaches reduce computational consumption, they may miss an optimal pixel pair when the number of available high-quality pixel pairs is limited. To address this shortcoming, we propose a novel multi-criterion sampling strategy that avoids missing high-quality pixel pairs by incorporating multi-range pixel pair sampling and high-quality samples selection method. This strategy is employed to develop a multi-criterion matting algorithm via Gaussian process, which searches for the optimal pixel pair by using the Gaussian process fitting model instead of solving the original pixel pair objective function. Experimental results demonstrate that our proposed algorithm outperforms other methods even with 1% computing resources, and achieves alpha matte results comparable to those yielded by the state-of-the-art optimization algorithms.

Keywords: computing resources; Gaussian process fitting model; multi-criterion sampling strategy; high-quality pixel pairs; alpha matte

0. Introduction

Image matting is a crucial image processing technique with extensive applications in image synthesis [1,2], video editing [3,4], live broadcasting [5], and film special effects [6,7]. In image matting, alpha mattes can accurately extract foreground objects and merge with new backgrounds to render new scenes [34]. The concept of the alpha matte was first proposed by Thomas in 1984 [8], whereby an alpha matte estimation model was constructed by introducing the alpha channel. Mathematically, the color value I_p , including RGB, of a pixel p can be linearly represented by the foreground color F_p and the background color B_p in the original image, as shown in Equation (1):

$$I_p = \alpha_p F_p + (1 - \alpha_p) B_p \tag{1}$$

where α_p is the alpha matte of the foreground object at pixel p , and $\alpha_p \in [0, 1]$. Specifically, α_p takes 1 when p belongs to the foreground, it is assigned the value of 0 when p belongs to the background, and is assigned a specific value in the range $(0, 1)$ when p is a semi-transparent pixel of which the color is a mixture of a foreground pixel color and a

background pixel color. As both F_p and B_p are three-dimensional unknown vectors and α_p is an unknown scalar, Equation (1) is an ill-defined problem. In order to accurately determine the value of α , Rhemann et al. [9] introduced a trimap, which divides the image into three non-overlapping regions, denotes as known foreground, known background and unknown regions, to impose additional constraints on the image matting problem, as shown in Figure 1 (where F is the foreground region with $\alpha = 1$, B is the background region with $\alpha = 0$, and U is the unknown region with α in the range $(0, 1)$).

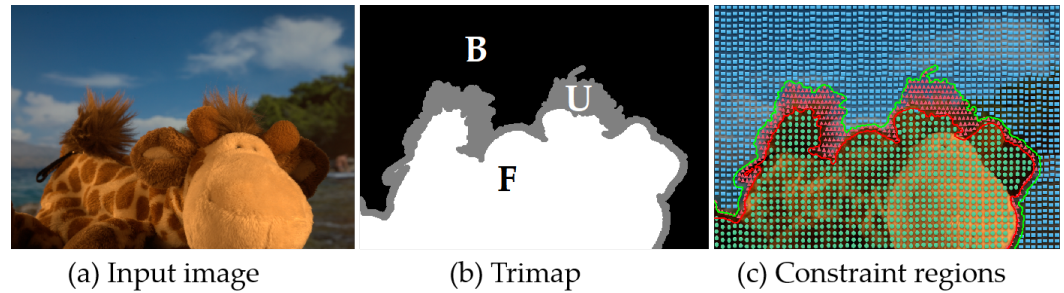


Figure 1. Image and trimap

Pixel pair optimization-based matting method is a class of competitive image matting approaches that offer significant advantages in terms of parallelization [10]. These methods are particularly effective in processing error-marked trimap [11] or foreground that is spatially disconnected [12–14]. Essentially, the natural image matting problem is transformed into a pixel pair optimization problem as shown in Equation (2).

$$\begin{aligned} \min f(x_p) \\ \text{s.t. } x_p = (x_i^F, x_i^B)^T \\ p \in U; x_i^F \in F; x_i^B \in B \end{aligned} \quad (2)$$

where $f(x_p)$ is the pixel pair evaluation function of unknown pixel p , U , F and B are the pixel sets of unknown, known foreground and known background regions, respectively; x_p is the pixel pair decision vector of pixel p ; and x_i^F and x_i^B represent pixels in the known foreground and background regions, respectively. Once the foreground and background colors are obtained by solving the pixel pair optimization problem, the alpha value of the pixel p can be estimated via the following expression:

$$\hat{\alpha}_p = \frac{(I_p - B_p)(F_p - B_p)}{\|F_p - B_p\|^2} \quad (3)$$

where $\|\cdot\|^2$ denotes the Euclidean norm of vector \cdot .

The pixel pair optimization-based matting methods can be further divided into sampling-based methods and evolutionary-optimization-based matting methods. Sampling-based methods [17,18] to evaluate the alpha value of the unknown region by collecting the known foreground and background pixels as candidate samples, which narrows the search range through different sampling strategies. Such as, Liang et al. [32] proposed a surrogate model based on natural image matting, which effectively reduces the computational resource consumption, by building on top of random sampling. However, this approach also faces the issue of potential loss of optimal pixel pair due to the random sampling strategy. The main drawback of these sampling-based methods stems from the significant likelihood of high-quality pixel pairs loss, resulting in unsatisfactory alpha mattes. To avoid this issue, He et al. [19] proposed a global sampling method that employs all pixel pairs as candidate samples to avoid the missing of high-quality pixel pairs. However, this approach also results in increased computational resource consumption. Then the evolutionary-optimization-based [35,36] methods are proposed, which can effectively

mitigate the drawback of high-quality pixel pairs loss in sampling-based methods and improve the quality of alpha mattes. For instance, Liang et al. [15] used the evolutionary algorithm instead of the pixel pair sampling process proposed a multiobjective evolutionary algorithm based on multi-criteria decomposition. This algorithm utilizes all available computing resources by adjusting the number of iterations of the evolutionary algorithm, and theoretically eliminates the risk of missing real samples. On the other hand, to address the problem of computing resource consumption, Liang et al. [16] developed a multi-scale evolutionary pixel pair optimization framework which transforms the large-scale pixel-pair optimization problem into multiple sub-optimization problems of different scales by using image pyramid. Although evolutionary-optimization-based methods utilizing various evolutionary algorithms have improved the accuracy of alpha matte, it may require thousands of iterations to find the optimal solution. Limited computing resources may restrict the applicability of this method and also compromise the quality of alpha mattes. In summary, neither the sampling-based method nor the existing evolutionary optimization-based method can provide satisfactory alpha mattes under limited computing resources. In image matting tasks, there is less discussion on matting under limited computing resources.

These limitations have motivated the present study, as a part of which we designed a multi-criterion sampling strategy (MCSS) to ensure that high-quality pixel pairs are sampled. Furthermore, to reduce the consumption of computing resources, multi-criterion matting algorithm via Gaussian process (GP-MCMMatting) is proposed, which can provide a satisfactory alpha matte even when computing resources are limited. The contributions of the work presented in this paper are threefold:

- The problem of missing high-quality pixel pairs is alleviated by combining different features in a MCSS.
- Departing from the approaches adopted in traditional matting methods which rely on one evaluation function only, we combine multiple evaluation functions to comprehensively evaluate pixel pairs in order to select those that are of high quality, thus avoiding the limitation of a single evaluation function.
- To ensure that the matting problem can be solved even with limited computing resources, we adopt a new perspective and propose a novel GP-MCMMatting algorithm, whereby we employ Gaussian process fitting model (GPFM) instead of objective function to search for the optimal pixel pair. With this algorithm, we can achieve effective and accurate matting even with just 1% of the computing resources.

Next, a description of the algorithm proposed in this article will be presented. The article consists of three sections: Section 1 covers related work, Section 2 outlines the problem description, and Section 3 introduces the GP-MCMMatting algorithm, which includes the MCSS in Section 3.1 and the Gaussian process fitting model in Section 3.2. The related work in this field will be presented first.

1. Related Work

Recently, the field of image matting has experienced significant advancements, as reflected by numerous publications that can be broadly categorized into those related to sampling-based methods and evolutionary-optimization-based methods, respectively. In the brief literature review provided below, we will focus on the work most closely related to this article.

Sampling-based methods: Sampling-based methods take the sample pixel pairs of the known regions as the candidate sample, and select the optimal foreground-background pixel pair through the evaluation function to solve the alpha matte. For example, to avoid the loss of real samples, Feng et al. [20] clustered foreground/background regions and selected representative pixels in each class as candidate samples. Inspired by image inpainting, Tang et al. [18] combined sampling with deep learning methods, and used the image inpainting network to select foreground-background pixel pairs as candidate samples to evaluate the alpha mattes of unknown regions. As a part of their research, Huang et al. [21] designed a discrete multi-objective optimization algorithm based on pixel-

level sampling. They thus effectively solved the problems of incomplete sampling space and optimal sample loss in the super-pixel sampling method, and ensured the accuracy of alpha matte. The strategy adopted by Cao et al. [22] was rooted in the patch-based image matting method, as these authors used a patch-based adaptive matting algorithm for high-resolution images and videos. As shown in their work, this algorithm extends the adaptive framework to video matting and reduces the consumption of computer resources. In short, in sampling-based methods, different sampling strategies [23–25] are utilized to select the sample pixel pairs, which reduces the scale of the decision space as well as the computational resource consumption. However, when there are few high-quality pixel pairs in the input image, the sampling-based methods may not identify the optimal pixel pair, resulting in an unsatisfactory alpha matte extraction accuracy.

Evolutionary-optimization-based methods: Most evolutionary-optimization-based methods [33] are based on the assumption that adjacent pixels have similar alpha values. For example, Liang et al. [26] modeled the image matting problem as a combinatorial optimization problem in which foreground and background pixel pairs are assumed to be known. These authors designed a heuristic optimization algorithm based on adaptive convergence speed controller, which alleviated the problem of premature algorithm convergence when solving for the optimal pixel pair. In their work, Feng et al. [27] focused on addressing the large-scale problem of high-definition images, and proposed a competitive swarm optimization algorithm based on group collaboration to realize the group collaborative solution of large-scale combinatorial optimization problems. These authors demonstrated that, compared with the sampling-based method, the evolutionary-optimization-based method can effectively improve the alpha matte estimation accuracy. However, when this method is adopted, more than 5×10^3 pixel pairs need to be evaluated for each unknown pixel to ensure that high-quality pixel pairs are captured. Therefore, when the computing resources are limited, it is difficult to attain an adequate alpha value.

In summary, when computing resources are limited, it is difficult to obtain a desired matting result with the existing evolutionary-optimization-based and learning-based matting methods. Therefore, in this work, we propose a sampling-based multi-criterion sampling strategy (MCSS) to avoid the loss of high-quality pixel pairs. In addition, to achieve adequate matting with limited computing resources, we propose a novel algorithm—multi-criterion matting algorithm via Gaussian process (GP-MCMatting)—incorporating the MCSS. GP-MCMatting algorithm uses Gaussian process fitting model (GPFM) instead of the original objective function to search for the optimal pixel pair, which effectively achieves matting under limited computing resources while ensuring the desired matting accuracy.

2. Problem Description

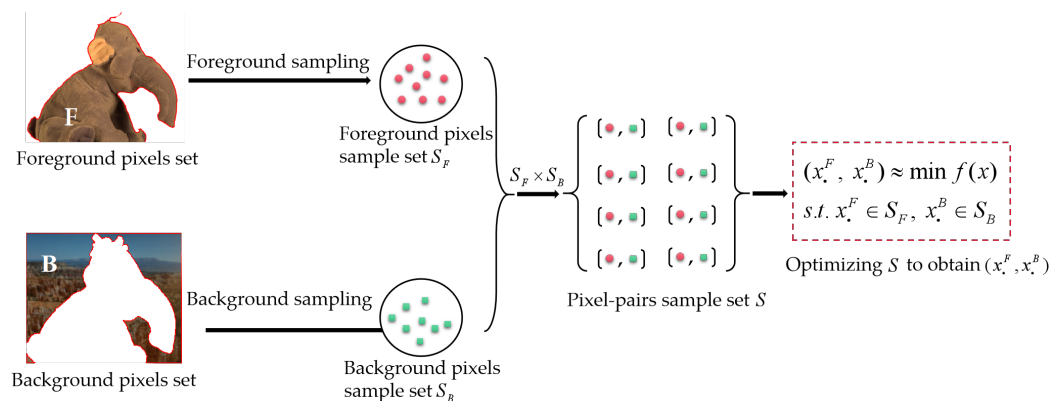


Figure 2. An example of a sampling-based matting method.

The authors of the existing sampling-based matting methods utilize different strategies to select samples from the known regions to obtain candidate samples for pixels in the unknown region, thereby evaluating the alpha matte of the unknown region. One such sampling method is shown in Figure 2.

In the image above, I represents an RGB image, and F, B, U correspond to the known foreground, background and unknown regions in the trimap respectively. S is the decision space composed of foreground and background samples which denotes $S_F \times S_B$. Finally, the evaluation function is used to determine the fitness value of each pixel pair, and the pixel pair with the best fitness is selected as the optimal pixel pair x_{opt} , based on the criteria shown in Equation (4):

$$\begin{aligned} \min f(x) &= (x^F, x^B) \\ \text{s.t. } x &\in U; (x^F, x^B) \in S \\ S &= S_F \times S_B \end{aligned} \quad (4)$$

where $f(*)$ is the evaluation function of the foreground-background pixel pair, x denotes unknown pixel in the unknown region, (x^F, x^B) represents the decision variable corresponding to the pixel in the known foreground and background regions, and $S_F \times S_B$ is the Cartesian product of the foreground and background sample sets.

As the dimensions of the candidate sample obtained by sampling are smaller than those of the original decision space, sampling-based method reduces the consumption of computing resources to a certain extent. However, when the number of high-quality pixel pairs in natural images is small (as shown in Figure 3), this strategy is prone to lose high-quality pixel pairs, resulting in unsatisfactory matting quality.



Figure 3. Case with a small number of high-quality pixels in the original image.

As shown in Figure 3, depicting GT16 from the alphamattng dataset (with a 800×536 size), for the flag of the unknown region to be solved, there are fewer than 500 high-quality pixels confined to a smaller region. Thus, the probability of high-quality pixels being sampled is 0.0034. The sampling strategy proposed in this work that can be adopted to overcome this issue is described below.

3. Multi-criterion matting algorithm via Gaussian process

In this section, we will introduce GP-MCMMatting algorithm which mainly consists of two stages: (1) multi-criteria sampling strategy (MCSS); (2) Gaussian process fitting model (GPFM).

3.1. Multi-Criterion Sampling Strategy

This subsection details the multi-criterion sampling strategy (MCSS), which consists of (1) multi-range pixel pairs sampling and (2) high-quality samples selection.

3.1.1. Multi-range pixel pairs sampling

Sampling-based methods rely on local or global sampling strategies to sample pixel pairs, whereby the former approaches risk missing high-quality pixel pairs. In order to compensate for this shortcoming, when the latter strategy is adopted, all foreground and background pixel pairs are treated as the sample set to ensure that the optimal solution is found. While this avoids the loss of real samples, it also increases the consumption of computing resources. In this work, we mitigate the aforementioned shortcomings by assuming that there is an optimal pixel pair region in the input image, due to which high-quality pixel pairs can be identified by sampling this region. Guided by this assumption, we designed a multi-range pixel pair sampling method based on the color and spatial position of pixels.

In multi-range pixel pairs sampling, the color similarity score between pixels can be reformulated as follows:

$$D^c = \|I_p - I_i^U\|_2, I_p \in F \cup B \quad (5)$$

where $\|\cdot\|_2$ denotes Euclidean norm of vector*, $F \cup B$ represents the set of known regions, I_p is the color value of known pixel p , and I_i^U is the color value of the unknown pixel i .

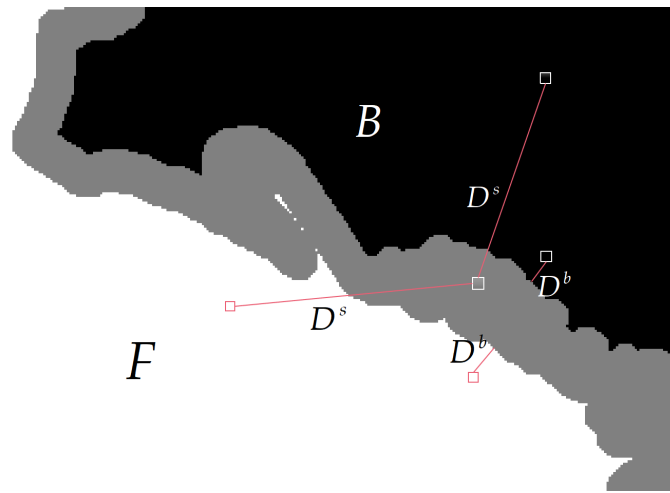


Figure 4. Spatial distance between pixels.

In image matting, the spatial position of pixels can reflect their structural features which may help in the differentiation among pixels. For this purpose, the similarity between the unknown region and the known boundary pixels, as well as the similarity between the unknown region and the long-range known regions (as shown in Figure 4), are calculated using the expressions shown below:

$$D^s = \|I_{p,in} - I_{i,in}^U\|_2, I_{p,in} \in F_{in} \cup B_{in} \quad (6)$$

$$D^b = \|I_{p,in}^b - I_{i,in}^U\|_2, I_{p,in}^b \in F_{in} \cup B_{in} \quad (7)$$

where D^s denotes the spatial position distance between the unknown pixels and the long-range known pixels; D^b represents the spatial distance between the pixels in the unknown region and the pixels in the known boundaries; $I_{p,in}^b$ represents the coordinate index values of the pixels in the known boundaries, $I_{p,in}$ denotes the coordinate index value of pixels in the long-range known region; $I_{i,in}^U$ denotes the coordinate index value of the unknown pixel, and $F_{in} \cup B_{in}$ is the coordinate space of the known regions.

Let the color distance set between the unknown pixels and the known pixels be given by $D^c = \{D_1^c, D_2^c, \dots, D_m^c\}$, whereas the spatial distance between the unknown pixels and the long-range known region pixels is given by $D^s = \{D_1^s, D_2^s, \dots, D_m^s\}$, and

the spatial distance between the unknown pixels and the pixels in the known boundaries is $D^b = \{D_1^b, D_2^b, \dots, D_m^b\}$. For a more intuitive view of the pixel distance scores, these three sets are rearranged in ascending order, i.e., $D_{(\cdot)}^c = \{D_{(1)}^c, D_{(2)}^c, \dots, D_{(m)}^c\}$, $D_{(\cdot)}^s = \{D_{(1)}^s, D_{(2)}^s, \dots, D_{(m)}^s\}$, and $D_{(\cdot)}^b = \{D_{(1)}^b, D_{(2)}^b, \dots, D_{(m)}^b\}$. According to the sample sets of three different distances, the color is first used as the main collection feature, after which the pixels with similar colors and close distances in the set are considered as the first type of candidate samples. Thus sampling process is described by the following expressions:

$$X^c = \begin{cases} X^c \cup S_k^c, & S_k^c < \frac{d * \max(S^c)}{|S^c|}, k = 1, 2, \dots, |S^c| \\ \emptyset, & \text{other} \end{cases} \quad (8)$$

$$S^c = \begin{cases} S^c \cup \{D_{(j)}^s\} \cup \{D_{(j)}^b\}, & \text{if } D_{(j)}^c < \varepsilon \\ \emptyset, & \text{other} \end{cases}, j = 1, 2, \dots, |D_{(\cdot)}^c| \quad (9)$$

where X^c is a sample set with similar color and close distances, whereas S^c is the set of similar color pixels with the unknown pixels, ε denotes the threshold of color distance, and $\frac{d * \max(S^c)}{|S^c|}$ represents the proportion of pixels with small color distance and coordinate space distance in S^c set, where d denotes the number of samples.

Furthermore, according to the obtained multi-range sets, the coordinate space is the main acquisition feature, and the pixels in the same set characterized by close spatial distance and similar color are considered as the second candidate sample type. This sampling method is described by the following equations:

$$X^s = \begin{cases} X^s \cup S_k^s, & S_k^s < \frac{d * \max(S^s)}{|S^s|}, k = 1, 2, \dots, |S^s| \\ \emptyset, & \text{other} \end{cases} \quad (10)$$

$$S^s = \begin{cases} S^s \cup \{D_{(j)}^c\}, & \text{if } D_{(j)}^s < d \\ \emptyset, & \text{other} \end{cases}, j = 1, 2, \dots, |D_{(\cdot)}^s| \quad (11)$$

where X^s is a sample set with close spatial distance and similar color, and S^s represents the set of similar pixel distances. Thus, when sampling based on different primary features, the sample sets X^c and X^s are formed, allowing the final candidate sample X to be obtained as their union, i.e., $X = X^c \times X^s$ which is the Cartesian product of X^c and X^s .

3.1.2. High-quality samples selection

As explained in the preceding section, multi-range pixel pair sampling yields the candidate sample set $X = X^c \times X^s$. In cases with a large number of candidate samples that need to be considered for obtaining high-quality pixel pairs, a high-quality sample selection method proposed here can be adopted, which is combined with the multi-range pixel pair sampling method to form MCSS.

In the process of pixel pair evaluation, a single evaluation function is usually used to evaluate the optimal pixel pair. However, this may compromise the ability to determine the fitness value of a given pixel pair [27]. Therefore, we propose a novel approach that combines multiple evaluation functions to select high-quality pixel pairs as candidate samples. Specifically, we employ color difference evaluation $f_c(x)$, fuzzy evaluation $f_f(x)$, and fuzzy multi-criterion evaluation $f_m(x)$ as joint evaluation indices for sample assessment. Let f_i denotes the fitness value after averaging the three evaluation functions of pixel x . Accordingly, the fitness value corresponding to the elements in candidate sample X is $F = \{f_1, f_2, \dots, f_{|X|}\}$, where $f_i = 1/3 \sum (f_c(x) + f_f(x) + f_m(x))$. Reordering F in ascending order yields $F_{(\cdot)} = \{f_{(1)}, f_{(2)}, \dots, f_{|X|}\}$. Then, according to the fitness value obtained by the

joint evaluation function, the high-quality pixel pairs can be selected using the expression below:

$$\Omega = \begin{cases} \Omega_f \cup f_i, & \text{if } \min f_i(x) + 1 > f_i(x), i = 1, 2, \dots, |F|, f_i \in F \\ \emptyset, & \text{other} \end{cases} \quad (12)$$

$$\Omega_f \rightarrow \Omega \quad (13)$$

where Ω_f represents the set of the high-quality pixel pairs fitness values; Ω is the pixel information corresponding to the fitness values of high-quality pixel pairs; and $\min f_i(x) + 1 > f_i(x)$ is a threshold set to eliminate excessive fitness values. After obtaining high-quality pixel pairs according to Equation (12), (13), the number of high-quality pixel pair samples is far smaller than the number of pixels in the decision space. As shown in Algorithm 1, the aforementioned approaches are combined to yield MCSS.

Algorithm 1 : Multi-criterion sampling strategy.

Input: image and trimap.

1. // For information on image pixel.
2. $F \cup B$ = Known pixel information by trimap.
3. **for** $i = 1$ **to** $|F \cup B|$ **do**
4. // multi-range pixel-pairs sampling.
5. $\{D^c, D^s, D^b\}$ = By Equation (5), (6), (7).
6. $\{D_{(\cdot)}^c, D_{(\cdot)}^s, D_{(\cdot)}^b\}$ = Sort the sets in ascending order.
7. **while** $D_{(\cdot)}^c < \varepsilon$ **do**
8. X^c = By Equation (8), (9).
9. **end while**
10. **while** $D_{(\cdot)}^s < d$ **do**
11. X^s = By Equation (10), (11).
12. **end while**
13. $X = X^c \times X^s$.
14. **end for**
15. // High-quality sample selection.
16. $F_{(\cdot)} = \{f_{(1)}, f_{(2)}, \dots, f_{(|X|)}\}$ = By Equation (12).
17. **if** stop criterion is not met **then**
18. $\Omega = \Omega \cup \{x_i\}$ // x_i is the corresponding sample pixel of f_i .
19. **end if**

Output: high-quality pixel pairs set Ω .

Specifically, to ensure that high-quality pixel pairs are not missing, in Line 1-2 foreground and background pixel information is gathered according to the input image, while in Line 3-14 the candidate sample set X is output after excessive range sampling, and in Line 15-19 the final high-quality samples set Ω is obtained according to the high-quality selection method.

3.2. Multi-criterion matting algorithm via Gaussian process

In this subsection, we will introduce the multi-criterion matting algorithm via Gaussian process (GP-MCMatting) proposed in this work, which enables image matting even when computing resources are limited while ensuring the required accuracy of image matting.

3.2.1. Gaussian process fitting model

The objective function of natural image matting problem is typically complex due to the simultaneous consideration of the similarity between pixels and the foreground/background regions, as well as the similarity among pixels. Traditional objective functions usually require nonlinear optimization algorithms for solving, which demands intensive computational resources and time [16]. When computing resources are limited, it may

be challenging to directly use traditional objective function-based methods. Accordingly, we assume that the optimal foreground and background pixel pair can be evaluated by fitting the parameters of the kernel function in the Gaussian process (GP), i.e., the solution of the pixel pairs original objective function can be approximately replaced by fitting the parameters of the GP using the following expressions:

$$\begin{aligned} \min H(x_{i,in}) &\rightarrow \min f(x) \\ \text{s.t. } \min f(x) & \\ x &= (x_i^F, x_i^B), x_{i,in} = (x_{i,in}^F, x_{i,in}^B) \\ x_i^F, x_{i,in}^F &\in F, F_{in}; x_i^B, x_{i,in}^B \in B, B_{in} \end{aligned} \quad (14)$$

where $H(x_{i,in})$ is the Gaussian process fitting model (GPFM). Due to there are many redundant solution space regions in the coordinate space, in the proposed algorithm, the image index number space is used to construct the distribution of the objective function. Moreover, to avoid crossing the boundary when searching for the optimal solution, the GPFM is constructed in the index value space.

GP is an infinite set of random variable distributions, where the joint distribution function of each finite subset is subject to Gaussian distribution [28,29]. Therefore, the GP is completely determined by the mean function and covariance kernel function between any two random variables [30,31]. In this work, the optimization of the GPFM model is achieved by approximating the optimal solution of the pixel pair objective function, essentially by estimating the undetermined parameters in the GPFM and then using the evaluated parameters to obtain the optimal solution [32]. Let θ and $\hat{\theta}$ denote the parameter vector and the estimated parameter vector of the kernel function in the GPFM, respectively. Then the likelihood function is used to estimate the kernel function parameters in the Gaussian process fitting model. Mathematically, the expression can be described as follows:

$$\hat{\theta} = L(\theta|f(x), x_{i,in}) = \arg \min_{\theta} \log P(f(x), x_{i,in}|\theta) \quad (15)$$

Therefore, According to Equation (15), the GPFM of the pixel pair evaluation function can be obtained via the following expressions:

$$\min H = H(x_{i,in}|\hat{\theta}) \quad (16)$$

Then the index position of the optimal pixel pair can be evaluated by fitting GPFM in the Equation (16), allowing us to solve for the optimal pixel pair.

3.2.2. Multi-criterion matting algorithm via Gaussian process

Natural image matting is a large-scale problem, due to which extensive computing resources are needed to solve the original objective function directly. Therefore, to achieve matting with limited computing resources, we propose a novel matting algorithm named multi-criterion matting algorithm via Gaussian process (GP-MCMatting), which includes (1) multi-criterion sampling strategy (MCSS) and (2) Gaussian process fitting model (GPFM). The former is mainly used to select high-quality sample pixel pairs from a large number of decision variables. The latter mainly uses GPFM to approximate the original objective function of natural images based on the MCSS, thereby reducing the consumption of computational resources. For constructing the GPFM basis, we define Θ which is a penalty function of GPFM described as:

$$\Theta(\Omega, \gamma) = h(\Omega) - \gamma \sum \log \Omega \quad (17)$$

where γ is the attenuation factor of the penalty function, and Ω is the set of high-quality pixel pair samples.

Once the GPFM is constructed, it is utilized to approximate the original objective function for a given pixel pair, allowing the optimal pixel pair to be obtained by solving the

extreme points of the model via the high-quality pixel pair set Ω . In this work, the optimal solution of GPFM is obtained based on the ideas behind the interior-point algorithm (IPA). Within the solving process, the optimal solution x_{min} of GPFM is approximately equivalent to the optimal solution x_{best} of the objective function. In addition, we find that the optimal pixel pair is usually located in the X^{loc} of the known region closest to the unknown pixels. Therefore, selecting the closest pixel pair in the local foreground region and the background region as the initial IPA population often yields a viable solution. When this assumption does not hold, the IPA algorithm can also find the optimal foreground-background pixel pairs by solving the GPFM, because the algorithm is applied to the entire search space, thus theoretically avoiding the loss of the optimal pixel pair. The solving process of GPFMCMatting is shown in Algorithm 2.

Algorithm 2 : Multi-criteria matting algorithm via Gaussian process.

Input: image and trimap.

1. //Initialize parameters ϵ, τ .
2. $x^{loc} = X^{loc}(x)$.
3. γ_k =Generate a random number greater than 0.
4. c = Generate a random number between $[0,1]$.
5. **for** $i = 1$ **to** $|U|$ **do**
6. //Gaussian process fitting model construction.
7. Ω =According to the Algorithm 1.
8. $(f(x), x_{i,in}) = \Omega$.
9. $H = H(L_p(\theta|f(x), x_{i,in})), x_{i,in} \in \Omega$.
10. //Optimal pixel pair estimation.
11. $x_{min} = \min H(x^{loc})$.
12. **while** $\epsilon > \tau$ **do**
13. $x_{\gamma_k} = \frac{\partial \Theta}{\partial x_{\gamma_k}}$.
14. $\tau = \left\| \frac{\Theta(x_{\gamma_k}^{init} - \gamma_k) - \Theta(x_{\gamma_{k-1}}^{init} - \gamma_{k-1})}{\Theta(x_{\gamma_{k-1}}^{init} - \gamma_{k-1})} \right\|$.
15. $\epsilon = \|x_{\gamma_k} - x^{init}\|$.
16. $x^{init} = x_{\gamma_k}$.
17. $\gamma_k = \gamma_{k-1} \cdot c$.
18. **if** $\gamma_k \leq 0$ **then**.
19. γ_k = a random number greater than 0.
20. c = a random number between $[0,1]$.
21. **end if**
22. **end while**
23. **end for**
24. $x_{best} = x_{\gamma_k}$.

Output: x_{best} .

Specifically, let ϵ represents the distance between GPFM and the target function that needs to be approximated, τ is a small value obtained from a penalty function. $\frac{\partial \Theta}{\partial x_{\gamma_k}}$ is the partial derivative, where c is a randomly generated attenuation factor, and γ_i is a random penalty coefficient greater than 0. Ω is a set of high-quality pixel pairs obtained by Algorithm 1. In Algorithm 2, the required parameters are first initialized, and lines 5-10 are used to construct GPFM. Lines 12-22 are the process of solving the optimal solution of GPFM. The algorithm stops iterating when the optimal solution of GPFM is approximately equivalent to the optimal solution of the objective function.

4. Experiments and Results

In this section, three sets of experiments are described, which were performed to verify the effectiveness of the high-quality pixel pairs selection strategy and the effectiveness of the algorithm.

4.1. Experimental setup

In the experiments, the alphamattting dataset presented by Rhemann et al. [9] (which contains 35 images, 27 of which are training images and 8 are testing images) was used as the benchmark dataset. All experiments were run on Intel (R) Core (TM) i7-9700 3.00GHz CPU, 16G memory server. Based on the experimental environment, we set up three groups of experiments, as outlined below.

- This experiment was mainly performed to verify that MCSS can effectively avoid the loss of high-quality pixel pairs, thus improving the matting performance.
- In this experiment, comparative analysis between GP-MCMatting and the state-of-the-art evolutionary optimization-based algorithms was conducted, such as pyramid matting framework (PMF) [16], adaptive convergence speed controller based on particle swarm optimization (PSOACSC) [26], and multiobjective evolutionary algorithm based on multi-criteria decomposition (MOEAMCD) [15], on the 1%, 2%, 5%, 10%, 20% and 100% computing resources basis. The matting performance of the proposed algorithm under limited computing resources was verified.
- This experiment was conducted to compare the GP-MCMatting performance with the aforementioned algorithms based on the availability of only 1% computing resources to verify its superiority.

In order to ensure the comparability of the experimental results based on different algorithms and facilitate statistical analysis of their performance, mean square error (MSE) and absolute value error (SAD) were adopted as evaluation indices. In the sections that follow, the results and analyses of each group of experiments are presented.

4.2. Effectiveness of multi-criterion sampling strategy

In the MCSS, the spatial coordinates and color features of pixels are sampled by solving Equation (8)-(9). In Equation (9), pixels whose color distance is less than ϵ are considered as candidate samples. In order to determine the optimal value of color distance parameters, we calculate the matting results under different distances. Figure 5 shows the sum of MSE values of 27 alphamattting training sets based on 1% computing resources and different color distance parameters. The results show that, when the color parameter is assigned the value of 10 (the red corresponds to the dashed line), the total MSE based on all 27 images is the smallest with a value of 0.789, i.e., the alpha matte accuracy is the highest. Therefore, the color distance parameter ϵ is set to 10 in the MCSS.

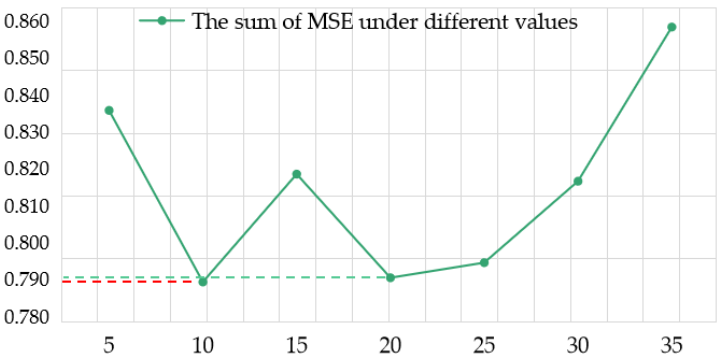


Figure 5. Sensitivity analysis of the color distance parameter.

Table 1. Comparison of the matting results yielded by different evaluation functions.

	Color difference evaluation function	Multiobjective evaluation function	Fuzzy evaluation function	Multi-criteria sampling strategy
MSE	0.0299	0.0297	0.0293	0.0292
SAD	7.2699	7.1731	7.1628	7.0999

Additionally, to verify the effectiveness of the high-quality samples selection method in the MCSS, a comparative analysis on the matting quality obtained by selecting different evaluation functions was performed and the findings are shown in Table 1. The comparisons are based on the sum of MSE and SAD of 27 images solved by different evaluation functions. By referring to Table 1, we can see that on the basis of the MSE and SAD evaluation metrics, the MCSS outperforms the method based on a single evaluation function. Therefore, the experimental results show that the combination of multiple evaluation functions to select high-quality pixel pairs is significantly better than a single evaluation function to select pixel pairs, which fully verifies the effectiveness of MCSS.

4.3. Algorithm evaluation and comparison under the conditions characterized by limited computing resources

In this subsection, GP-MCMMatting is compared with the state-of-the-art evolutionary optimization-based algorithms to verify the matting performance of the proposed algorithm when computing resources are limited. As most algorithms require 5000 iterations per pixel [15,16,26], this was adopted as the benchmark, and 1%, 2%, 5%, 10%, 20%, and 100% of 5000 computing resource availability is considered in different scenarios to compare the matting performance of studied algorithms. For the fairness of comparison, MSE and SAD are used as the evaluation indicators to compare the alpha matte accuracy of different algorithms. The results in Table 2 represent the sum of MSE and SAD of different algorithms when applied to the training sets contained in the alphamatting dataset under different computing-resource conditions.

Table 2. The SAD and MSE values for the GP-MCMMatting and the state-of-the-art evolutionary optimization-based algorithms based on their application to 27 images at the 1%, 2%, 10%, 20% and 100% computer power and 5000 evaluations. Bold Arabic numerals indicate the index with the highest ranking.

Computing resources	SAD					
	1%	2%	5%	10%	20%	100%
PSOACSC[26]	604.425	604.267	604.418	604.137	603.950	602.987
MOEAMCD[15]	243.965	243.346	242.741	242.179	243.028	242.741
PMF[16]	349.160	321.151	294.067	272.818	253.481	228.433
Ours	191.697	187.752	202.500	214.409	216.114	210.910

Computing resources	MSE					
	1%	2%	5%	10%	20%	100%
PSOACSC[26]	5.061	5.063	5.063	5.062	5.056	5.039
MOEAMCD[15]	1.127	1.121	1.113	1.116	1.118	1.113
PMF[16]	2.231	1.910	1.689	1.430	1.257	1.028
Ours	0.789	0.826	1.029	1.151	1.163	1.171

According to the results reported in Table 2, in terms of the SAD value, the matting performance of the proposed algorithm under limited and sufficient computing resources is superior to that associated with PMF, MOEAMCD and PSOACSC algorithms. According to the MSE evaluation index, the matting effect of the proposed GP-MCMMatting algorithm is better than that of the algorithms used in comparisons only when 1%, 2% and 5% of the computing resources are considered. Nonetheless, GP-MCMMatting algorithm is still

superior to PMF and PSOACSC in the scenarios based on 10%, 20% and 100% computing resource availability. When both SAD and MSE are considered, however, the proposed GP-MCMatting algorithm not only achieves competitive matting effects under limited computing resources, but can also achieve good results even when computing resources are sufficient. Thus, the proposed algorithm based on the MCSS effectively realizes the matting results irrespective of the computing resource availability.

In order to further analyze the effectiveness of GP-MCMatting under limited computing resources, the MSE results of different algorithms are compared based on their application on 27 images in the alphamatting dataset and availability of 1% computing resources.

4.4. Comparison to the state-of-the-art methods

In order to demonstrate the effectiveness of the proposed GP-MCMatting algorithm and compare its performance to the state-of-the-art algorithms when computing resources are limited, MSE values obtained by applying different matting algorithms to 27 training sets under 1% computing resources are shown in Table 3.

According to the results reported in Table 3, GP-MCMatting outperforms PMF, PAO-ACSC and MOEAMCD algorithms in 24 of the 27 cases (i.e., with the exception of GT09, GT24 and GT15 images). The reasons behind its suboptimal performance in these three cases will be analyzed in detail in Section 5.5.

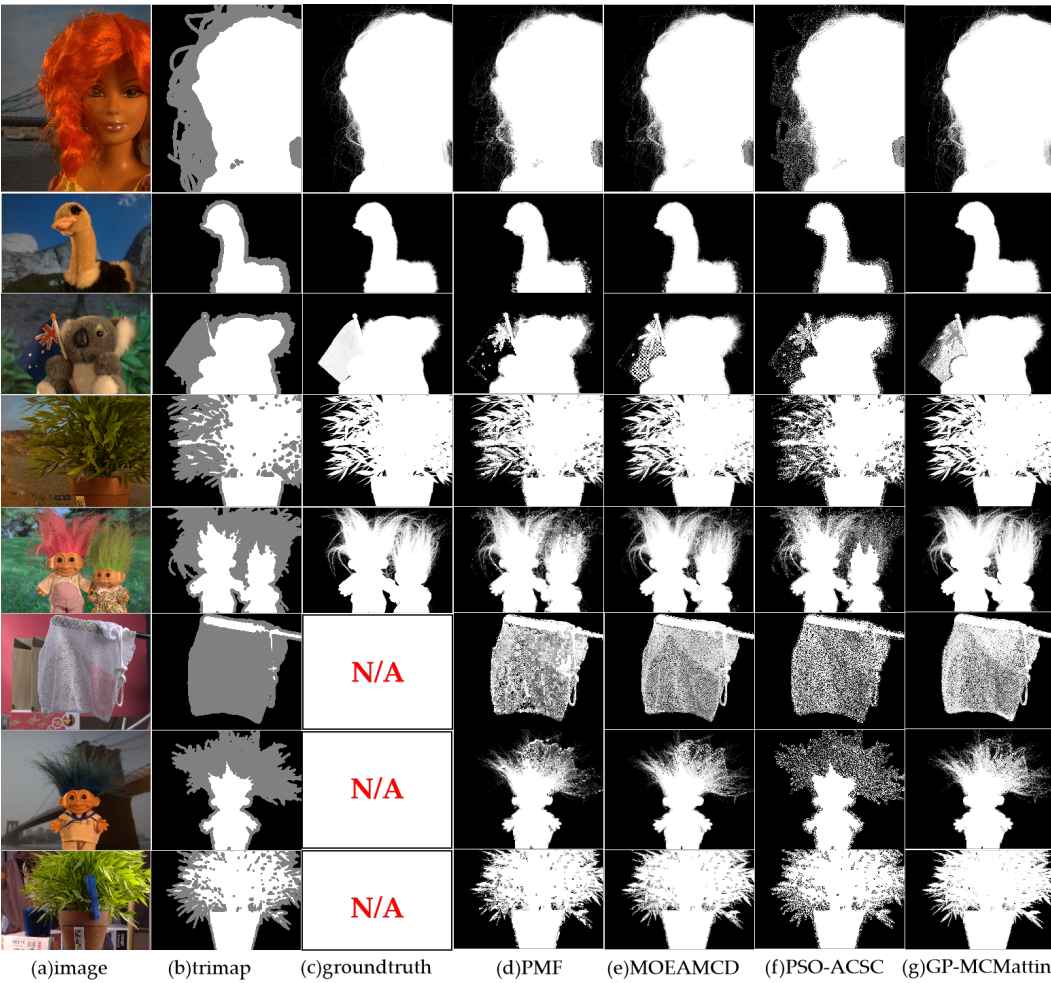


Figure 6. Visual comparison on the alphamatting dataset. (a) input image; (b) trimap; (c) ground truth; (d) PMF; (e) MOEA-MCD; (f) PSOACSC; (g) GP-MCMatting.

To further verify the matting effect of the proposed algorithm, the results yielded by the GP-MCMMatting algorithm on the training set and test set are depicted in Figure 6. It is evident that GP-MCMMatting effectively evaluates the object containing hair in the foreground target in the image (the visualization results in rows 1, 2, 3, 4 and 6). Conversely, according to the comprehensive visualization results and MSE accuracy results, the matting effect of the compared algorithms under the limited computing resources is not satisfactory, and there are large unknown areas that cannot be evaluated. Based on the analysis of the experimental results shown in Table 3 and the images included in Figure 6, it is evident that the algorithm proposed in this work avoids the loss of the optimal pixel pair by selecting high-quality pixel pairs, thus improving the extraction accuracy of the foreground mask. In addition, under limited computing resources, satisfactory matting is realized by approximately solving the GPFM, which reflects the superiority of the proposed GP-MCMMatting.

Table 3. The MSE values for GP-MCMMatting and the state-of-the-art evolutionary-optimization-based methods based on their application on 27 images under 1% computing resources. Bold Arabic numerals indicate the index with the highest ranking.

Algorithms	GT01	GT02	GT03	GT04	GT05	GT06	GT07	GT08	GT09
Ours	3.33E-03	6.40E-03	9.68E-03	1.23E-02	1.49E-02	1.49E-02	7.89E-03	3.93E-02	1.29E-02
PSOACSC[26]	6.65E-02	2.13E-01	5.35E-02	1.01E-01	1.62E-01	2.24E-01	9.11E-02	1.26E-01	1.57E-01
MOEAMCD[15]	7.49E-03	1.53E-02	1.19E-02	2.15E-02	2.53E-02	2.71E-02	1.08E-02	4.40E-02	1.11E-02
PMF[16]	1.74E-02	1.23E-01	1.45E-02	3.28E-02	4.78E-02	4.45E-02	2.84E-02	5.71E-02	2.16E-02

Algorithms	GT10	GT11	GT12	GT13	GT14	GT15	GT16	GT17	GT18
Ours	2.32E-02	3.21E-02	1.00E-02	1.23E-02	7.81E-03	5.04E-02	7.64E-02	1.22E-02	7.50E-03
PSOACSC[26]	2.22E-01	3.02E-01	4.61E-02	2.08E-01	1.55E-01	1.79E-01	3.62E-01	1.41E-01	2.04E-01
MOEAMCD[15]	2.77E-02	3.93E-02	1.47E-02	2.29E-02	2.61E-02	4.02E-02	1.87E-01	1.59E-02	1.66E-02
PMF[16]	6.36E-02	7.65E-02	1.84E-02	6.66E-02	5.37E-02	9.36E-02	3.43E-01	3.01E-02	6.15E-02

Algorithms	GT19	GT20	GT21	GT22	GT23	GT24	GT25	GT26	GT27
Ours	8.82E-03	7.56E-03	1.57E-02	7.15E-03	7.35E-03	9.84E-02	1.51E-01	5.95E-02	8.06E-02
PSOACSC[26]	2.27E-01	7.33E-02	1.90E-01	1.19E-01	1.58E-01	3.54E-01	2.99E-01	2.56E-01	3.71E-01
MOEAMCD[15]	5.13E-02	1.21E-02	4.73E-02	1.38E-02	1.81E-02	6.88E-02	1.67E-01	6.94E-02	1.15E-01
PMF[16]	9.99E-02	1.34E-02	9.56E-02	2.61E-02	2.32E-02	1.05E-01	2.88E-01	1.64E-01	2.22E-01

4.5. Limitations of the GP-MCMMatting algorithm

The comparison and analysis of the experimental results in Sections 5.2-5.4 fully reflect the superiority of the proposed algorithm under conditions characterized by limited computing resources. However, the results reported in Table 3 in Section 5.4 show that the extraction accuracy of GP-MCMMatting algorithm is low when applied to the GT15 and GT24 images, and there are failures in the acquisition of high-quality pixel pairs, as shown in Figure 7.

The results depicted in Figure 7 reveal that the color information of the foreground and background pixels in the annotated region is relatively similar, as depicted by the green box in the images. Although the pixels in this region meet the color sampling requirements due to their minor color differences, the spatially close distribution of these pixels impedes the search for the optimal pixel pair during the evaluation of the kernel function parameters of Gaussian process field model (GPFM) using pixel spatial distribution. Consequently, in complex images that exhibit similar foreground and background characteristics, GPFM approximations cannot replace the original evaluation function when solving for the optimal pixel pairs. This fundamental limitation constrains the practical implementation of the GP-MCMMatting algorithm in such scenarios.

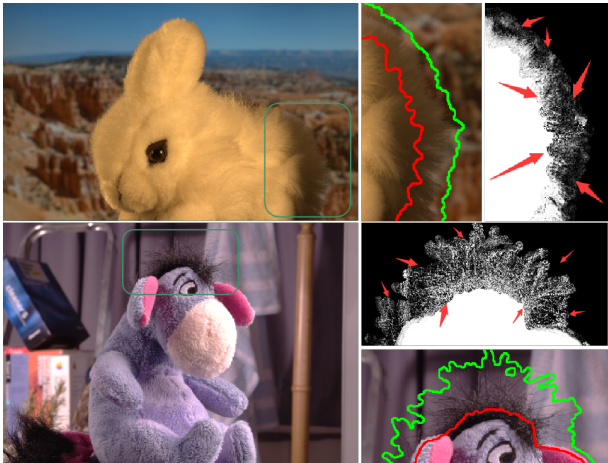


Figure 7. The case of GP-MCMatting failure when applied to the GT15 and GT24 images.

5. Conclusions

In this paper, we present a multi-criterion sampling matting algorithm via Gaussian process (GP-MCMatting) that effectively solves the matting problem with limited computing resources. To overcome the challenge of losing optimal pixel pair which is occurred in sampling-based methods, a MCSS was designed based on multi-range pixel pair sampling and high-quality samples selection. Additionally, to address the challenge of matting under limited computing resources, the GP-MCMatting algorithm searches optimal pixel pair using an approximation of the GPFM instead of the original evaluation function. This technique avoids the protracted calculations required by the original evaluation function while still ensuring accurate matting. The experimental results demonstrate that, the GP-MCMatting algorithm achieves similar results under sufficient computing resources and is superior when 1%, 2%, and 5% of computing resources are available.

However, the GP-MCMatting algorithm cannot be applied to input images with similar foreground and background color information. Therefore, these shortcomings will be addressed in future work.

Author Contributions: Conceptualization, F.F.-J and T.M.; Methodology, Y.Y. and G.H.-S; Software, G.H.-S and L.Y.-H; Validation, X.Y.; Formal analysis, F.F.-J; Investigation, T.M.; Resources, H.H.; Writing—original draft preparation, Y.Y.; Writing—review and editing, W.L., H.H., X.Y, F.F.-J, T.M. and L.Y.-H; Supervision, H.H.; Project administration, F.F.-J, T.M, L.Y.-H, X.Y. and H.H. All authors have read and agreed to the published version of the manuscript.

Acknowledgments: This work is supported by National Natural Science Foundation of China (62276103, 62002053, 61906069), the Guizhou Provincial Science and Technology Projects (QKHJCZK2022YB195, QKHJCZK2023YB143), Natural Science Foundation of Guangdong Province (2020A1515010696, 2022A1515011491, 2021A0101180005), the Fundamental Research Funds for the Central Universities (2020ZYGXZR014), the Youth Science and Technology Talents Cultivating Object of Guizhou Province (QJHKY2021104), the Science and Technology Support Program of Guizhou Province (QKHZC2021YB531), the Natural Science Research Project of Department of Education of Guizhou Province (QJJ2022015) and Guangdong Basic and Applied Basic Research Foundation (2019A1515111082) Zhongshan Science and Technology Research Project of Social welfare (2019B2010) High-level personnel Scientific Research Foundation Project of Zhongshan (2019A4018).

Data Availability Statement: The figures utilized to support the findings of this study are embraced in the article.

Conflicts of Interest: Declare conflicts of interest or state “The authors declare no conflict of interest.

References

1. Jiang, W.-H.; Yu, D.-D.; Xie, Z.-Z.; Li, Y.-Y.; Yuan, Z.-H.; Lu, H.-T. Trimap-guided Feature Mining and Fusion Network for Natural Image Matting. *Computer Vision and Image Understanding* **2023**, *230*, 1077–3142.

2. Huang, H.; Feng, F.-J.; Huang, S.; Chen, L.; Hao, Z.-F. Micro-scale Searching Algorithm for Coupling Matrix Optimization of Automated Microwave Filter Tuning. *IEEE Transactions on Cybernetics* **2023**, *53*, 2829–2840.

3. Hu, L.-P.; Kong, Y.-T.; Li, J.-D.; Li, X.-Q. Effective Local-Global Transformer for Natural Image Matting. *Journal IEEE Transactions on Circuits and Systems for Video Technology* **2023**, pp, 1–1.

4. Park, G.-T.; Son, S.-J.; Yoo, J.-Y.; Kim, S.-H.; Kwak, N. MatteFormer: Transformer-Based Image Matting via Prior-Tokens. In *Proceedings of the IEEE/CVF Conference on Computer Vision and Pattern Recognition* **2022**, pp, 11696–11706.

5. Lin, S.-C.; Yang, L.; Saleemi, I.; Sengupta, S. Robust High-resolution Video Matting with Temporal Guidance. In *Proceedings of the IEEE/CVF Winter Conference on Applications of Computer Vision* **2022**, pp, 3132–3141.

6. Sun, G.; Wang, Q.; Gu, C.; Tang, K.; Tai, Y.W. Deep Video Matting via Spatio-Temporal Alignment and Aggregation. In *Proceedings of the IEEE/CVF Conference on Computer Vision and Pattern Recognition* **2021**, pp. 6971–6980.

7. Yanan, S.; Tang, C.-K.; Tai, Y.-W. Semantic Image Matting. In *Proceedings of the IEEE/CVF Conference on Computer Vision and Pattern Recognition* **2021**, pp. 11120–11129.

8. Thomas, P.; Tom, D. Compositing Digital Images. *Proceedings of ACM Siggraph Computer Graphics* **1984**, *18*, 253–259.

9. Rhemann, C.; Rother, C.; Wang, J.; Gelautz, M.; Kohli, P.; Rott, P. A Perceptually Motivated Online Benchmark for Image Matting. In *Proceedings of the IEEE Conference on Computer Vision and Pattern Recognition*, Miami, FL, USA, **2009**, pp. 1826–1833.

10. Ding, H.; Zhang, H.; Liu, C.; Jiang, X. Deep Interactive Image Matting with Feature Propagation. *IEEE Transactions on Image Processing* **2022**, *31*, 2421–2432.

11. Liang, Y.-H.; Huang, H.; Cai, Z.-Q.; Hao, Z.-F.; Tan, K.-C. Deep Infrared Pedestrian Classification based on Automatic Image Matting. *Applied Soft Computing* **2019**, *77*, 484–496.

12. Chen, X.; Zou, D.; Zhao, Q.; Tan, P. Manifold Preserving Edit Propagation *ACM Transactions on Graphics* **2012**, *31*, 1–7.

13. Aksoy, Y.; Aydin, T.-O.; Pollefeys, M. Designing Effective Inter-pixel Information Flow for Natural Image Matting. In *Proceedings of the IEEE/CVF Conference on Computer Vision and Pattern Recognition* **2017**, pp. 29–37.

14. Li, X.; Li, J.; Lu, H. A Survey on Natural Image Matting with Closed Form Solutions. *IEEE Access* **2019**, *7*, 136658–136675.

15. Liang, Y.-H.; Huang, H.; Cai, Z.-Q.; Hao, Z.-F. Multiobjective Evolutionary Optimization Based on Fuzzy Multicriteria Evaluation and Decomposition for Image Matting. *IEEE Transactions on Fuzzy Systems* **2019**, *27*, 1100–1111.

16. Liang, Y.-H.; Feng, F.-J.; CAI, Z.-Q. Pyramid Matting: A Resource-Adaptive Multi-Scale Pixel-pair Optimization Framework for Image Matting. *IEEE Access* **2020**, *8*, 93487–93498.

17. Cai, Z.-Q.; Liang, L.; Huang, H.; Hu, H.; Liang, Y.-H. Improving Sampling-based Image Matting with Cooperative Co-evolution Differential Evolution Algorithm. *Applied Soft Computing* **2017**, *21*, 4417–4430.

18. Tang, J.-W.; Aksoy, Y.; Oztireli, C.; Gross, M.; Aydin, T.-O. Learning-based Sampling for Natural Image Matting. In *Proceedings of the IEEE/CVF Conference on Computer Vision and Pattern Recognition* **2019**, pp, 3055–3063.

19. He, K.-M.; Rhemann, C.; Rother, C.; Tang, X.-O.; Sun, J. A Global Sampling Method for Alpha Matting. In *Proceedings of the IEEE/CVF Conference on Computer Vision and Pattern Recognition* **2011**, pp. 2049–2056.

20. Feng, X.-X.; Liang, X.-H.; Zhang, Z.-L. A Cluster Sampling Method for Image Matting via Sparse Coding. In *European Conference on Computer Vision* **2016**, pp, 204–219.

21. Huang, H.; Liang, Y.-H.; Yang, X.; Hao, Z.-F. Pixel-level Discrete Multi-objective Sampling for Image Matting. *IEEE Transactions on Image Processing* **2019**, *28*, 3739–3751.

22. Cao, G.-Y.; Li, J.-W.; Chen, X.-H.; He, Z.-Q. Patch-based Self-adaptive Matting for High-resolution Image and Video. *The Visual Computer* **2019**, *35*, 133–147.

23. Shahrian, E.; Rajan, D.; Price, B.; Cohen, S. Improving Image Matting using Comprehensive Sampling Sets. In *Proceedings of the IEEE/CVF Conference on Computer Vision and Pattern Recognition* **2013**, pp, 636–643.

24. Wang, J.; Cohen, M.-F. Optimized Color Sampling for Robust Matting. In *Proceedings of the IEEE/CVF Conference on Computer Vision and Pattern Recognition* **2007**, pp, 1–8.

25. Eduardo, S.; Lopes, G.; Manuel, M.-O. Shared Sampling for Real-Time Alpha Matting. *Computer Graphics Forum* **2010**, *10*, 575–584.

26. Liang, Y.-H.; Huang, H.; Cai, Z.-Q. PSO-ACSC: A Large-scale Evolutionary Algorithm for Image Matting. *Frontiers in Computer Science* **2020**, *14*, 29–40.

27. Feng, F.-J.; Huang, H.; Wu, Q.-X.; Ling, X.; Liang, Y.-H.; Cai, Z.-Q. An Alpha Matting Algorithm based on Collaborative Swarm Optimization for High-resolution Images. *Journal Chinese Science : Information Science* **2020**, *50*, 424–437.

28. Rasmussen, C.E. Evaluation of Gaussian Processes and Other Methods for Non-Linear Regression. *Toronto, ON, Canada: Univ. Toronto* **1999**.

29. Rasmussen, C.E.; Williams, K.-I. *Gaussian Processes for Machine Learning (Adaptive Computation and Machine Learning)*, MIT Press: Cambridge, MA, USA, 2005.

30. Khan, M.-E.; Immer, A.; Abedi, E.; Korzepa, M. Approximate Inference Turns Deep Networks into Gaussian processes. *Advances in Neural Information Processing Systems* **2019**, pp, 3088–3098.

31. Zheng, Y.-J.; Yang, Y.-S.; Che, T.-T.; Hou, S.-J.; Huang, W.-H.; Gao, Y.; Tan, P. Image Matting with Deep Gaussian Process. *IEEE Transactions on Neural Networks and Learning Systems* **2022**.

32. Liang, Y.-H.; Gou, H.-S.; Feng, F.-J. Natural Image Matting based on Surrogate Model. *Applied Soft Computing* **2023**, *110*, 407, 1568–4946. 537

33. Feng, F.-J.; Huang, H.; Liu, D.; Liang, Y.-H. Local Complexity Difference Matting based on Weight Map and Alpha Mattes. *Multimedia Tools and Applications* **2022**, *81*, 43357–43372. 538

34. Li, J.-J.; Yuan, G.-J.; Fan, H. Robust Trimap Generation based on Manifold Ranking. *Information Sciences* **2020**, *519*, 200–214. 539

35. Rother, C.; Kolmogorov, V.; Blake, A. GrabCut: Interactive Foreground Extraction using Iterated Graph Cuts. *ACM Transactions on Graphics* **2004**, *23*, 309–314. 540

36. Levin, A.; Rav-Acha A.; Lischinski, D. Spectral Matting. *IEEE Transactions on Pattern Analysis and Machine Intelligence* **2008**, *30*, 1699–1712. 541

Disclaimer/Publisher’s Note: The statements, opinions and data contained in all publications are solely those of the individual author(s) and contributor(s) and not of MDPI and/or the editor(s). MDPI and/or the editor(s) disclaim responsibility for any injury to people or property resulting from any ideas, methods, instructions or products referred to in the content. 542